

Scattering of Oxygen Ions from Argon and Xenon*

J. G. KELLEY,† F. E. STEIGERT, AND W. W. WATSON
Yale University, New Haven, Connecticut

(Received February 6, 1962)

The forward-angle elastic scattering of 153-Mev oxygen ions from a natural argon target was measured and found to be compatible with the predictions of the sharp-cutoff model using a cutoff l value of 60 and a diffuseness parameter of 3.5. The forward-angle elastic scattering from a natural xenon target was similarly fitted, using a cutoff l value of 91. These would correspond to radius parameters r_0 of the order of 1.43 and 1.47 f, respectively. A survey of the reaction products observed in scattering O^{16} ions from a target of enriched Ar^{40} is also reported.

INTRODUCTION

IN recent months there have been several papers reporting the results of elastic scattering of heavy ions from light gas targets.¹⁻³ Almost invariably these have been in the region where the classical parameter η ($=Z_1Z_2e^2/hv$) has been less than 4. In this region, as was to be expected, the diffraction type of oscillations of cross section vs angle were the most prominent feature. In general, these results could only be parameterized well in terms of the positions of the extrema. The fits in terms of the absolute magnitudes were rather poor. While this is to be expected in the naive diffraction model calculation,⁴ one would hope that the sharp-cutoff model⁵ would give rather good agreement, particularly at the forward angles. Especially perplexing is the fact that several of the cross sections reported differ significantly from Coulomb even at the most forward angles observed. For example, both Smith³ and Newman¹ obtain the cross section for the C^{12} - N^{14} system at about 65 Mev in the center-of-mass system to be about two-thirds of Coulomb at 4° . On the opposite extreme, Smith reports the cross section for the C^{12} - C^{12} system at 60 Mev in the center-of-mass system to be almost 50% in excess of Mott predictions at 5° .

As one moves to heavier targets (or lower energy) the assumptions of the sharp-cutoff model will be better satisfied and one may expect better reproduction of the data. There has been considerable work reported in this region characterized by somewhat larger values of the parameter η .⁶⁻⁸ These results invariably show much

less oscillatory behavior, so that the only feature of the cross section to be accounted for is the location and shape of the cutoff. Thus the model would appear to do quite well. However, in most of these experiments it has been assumed that the cross section at forward angles is indeed equal to Coulomb in magnitude, with no attempt at an absolute calibration being made. The present paper reports the results of extending the earlier sequence of elastic scattering reactions to heavier gas targets in an attempt to observe the relative magnitudes of the cross sections as one moves into the more classical region. In this same vein, the previous results of scattering oxygen from natural neon have been reanalyzed for comparison to these heavier gases.

As an incidental part of the experiment, the fragments resulting from the bombardment of argon by oxygen ions were also observed. The preliminary analysis has been done in essentially the same manner as described by Roll.⁹

ELASTIC-SCATTERING APPARATUS

The experimental arrangement used was essentially the same as that described previously.¹⁻³ A magnetically analyzed beam of nominally 160-Mev oxygen ions was passed through a thin (2.65 mg/cm²) nickel gas-retaining foil into the gas-filled scattering volume. Collimation on the incident and scattered beams was sufficient to give angular resolutions of the order of 18 min at the most forward angles and 40 min at the remaining angles, where smaller yields were being encountered. In general the transition occurred at about 5° . Overlap of the order of 2° was taken to guarantee proper normalization. The scattered particles were observed in early experiments with a thin NaI crystal-DuMont 6292 phototube combination, and later with an RCA silicon junction detector. Unfortunately, in neither case was the resolution sufficient to split off contributions from the low-lying excited states of the target nuclei. An inelastic peak coming from the lowest lying levels of the projectile oxygen nucleus (approximately 7 Mev) was in both cases observed and resolved. The relative cross section was measured in terms of a particle-counting monitor observing reaction products at more backward angles. This was then later nor-

* This work was supported in part by the U. S. Atomic Energy Commission.

† Now at the Raytheon Company, Wayland, Massachusetts. Part of this work is from the doctoral dissertation of J. G. Kelley, submitted to the Graduate School, Yale University, May, 1960.

¹ E. Newman, P. G. Roll, and F. E. Steigert, Phys. Rev. **122**, 1842 (1961).

² P. G. Roll, E. Newman, and F. E. Steigert, Nuclear Phys. **29**, 544 (1962).

³ A. M. Smith, F. E. Steigert, Phys. Rev. **125**, 988 (1962).

⁴ G. Placzek and H. A. Bethe, Phys. Rev. **57**, 1075 (1940).

⁵ J. S. Blair, Phys. Rev. **108**, 827 (1957).

⁶ J. A. McIntyre, S. D. Baker, and T. L. Watts, Phys. Rev. **116**, 1212 (1959).

⁷ E. Goldberg and H. L. Reynolds, Phys. Rev. **112**, 1981 (1958).

⁸ A. Zucker and M. L. Halbert, in *Reactions Between Complex Nuclei*, edited by A. Zucker, E. C. Halbert, and F. T. Howard (John Wiley & Sons, Inc., New York, 1960), pp. 144.

⁹ P. G. Roll and F. E. Steigert, Nuclear Phys. **29**, 565 (1962).

malized by monitoring a run with the detector replaced by a Faraday cup set at 0° .

In the case of the argon scattering, commercial-grade gas was continually flowed through the chamber at a constant pressure of 50 mm of mercury. For the case of the xenon scattering, gas was sealed into the apparatus at 25 mm mercury pressure. The pressure and temperature were continuously monitored for assurance that light impurities were not accumulating from an air leak.

The energy at the scattering center was obtained by correction of the known momentum of the incident ions, using the nickel range-energy curves of Roll,¹⁰ an argon range-energy curve obtained expressly for the purpose with the assistance of Roll, and a calculated energy-loss curve for xenon using the relationships constructed by Northcliffe.¹¹ The approximate validity of the corrections could be checked by comparison with a similar reconstruction for the scattered ions. In the case of the crystal detectors the pulse-height-energy curves of Newman¹² were used for calibration. In the case of the junction detectors the response was assumed to be linear. The agreement between the predicted and the observed energy of the scattered ions was about 2%, which is basically the accuracy of the individual curves used.

Since, in general, the incident ions possessed more directivity than would be expected from a white source at the center of the beam-collimation slits, the mean beam direction could and did vary somewhat as a function of time. This possible ambiguity in angle was calibrated out by periodic measurements at a constant reference angle. Further control was obtained by continual alternation of positive and negative angles.

TABLE I. Estimated experimental errors.

	Small angles	Large angles
Counting statistics	$\pm 2\%$	± 2 to 3%
Monitor statistics	$\pm 1\%$	
Target density	$\pm 1.5\%$	
Geometrical correction	$\pm 0.5\%$	$\pm 1.5\%$
Background and slit-edge scattering	$\pm 0.5\%$	
Total relative error	$\pm 4\%$	$\pm 5\%$
Beam current	$\pm 3\%$	
Multiple scattering ^a	$+ 5\%$	
Total absolute error	$\pm 8\%$	$\pm 9\%$
Beam energy	$\pm 2\%$	
Angle	$\pm 2'$	$\pm 5'$
Error relative to Coulomb	$\pm 10\%$	$\pm 12\%$

^a Only important at forward angles, if at all.

¹⁰ P. G. Roll and F. E. Steigert, *Nuclear Phys.* **16**, 534 (1960).

¹¹ L. C. Northcliffe, *Phys. Rev.* **120**, 1744 (1960), and private communication.

¹² E. Newman and F. E. Steigert, *Phys. Rev.* **118**, 1575 (1960).

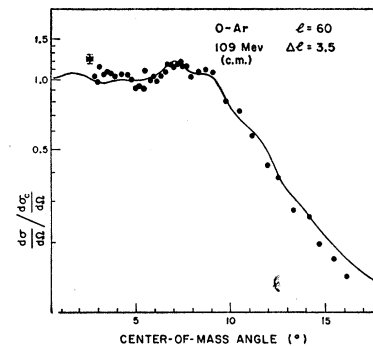


FIG. 1. Differential elastic scattering cross section relative to Coulomb vs center-of-mass angle for oxygen on argon at 109 Mev. Error bars designate probable relative errors among experimental points. Solid curve is diffused sharp-cutoff-model prediction for the parameters shown.

RESULTS AND DISCUSSION

The differential cross sections obtained are displayed in Figs. 1 and 2 as ratios to the Coulomb cross section. These data have already been corrected for the varying target thickness and for finite geometry according to the recipe of Critchfield and Dodder.¹³ The individual angles have also been adjusted for the slow drift of the mean beam axis during the course of the run. No other corrections or normalizations have been applied.

A summary of the probable errors is presented in Table I. Most of the entries are self-explanatory. To obtain the net probable errors, the contributing factors have been added in quadrature. Linear addition, to place extreme limits, would give ± 6 to 7% for the relative error, $+20\%$ and -15% for the absolute errors, and $+38\%$ and -23% for the apparent errors relative to Coulomb. Account has not been taken of multiple scattering in assessing the relative error, since this is strictly a small-angle effect and should only result in anomalously large cross sections at forward angles. Smith,³ using this same apparatus, reports no observable effects ascribable to this source. However, the present targets are considerably heavier and may be expected to show an enhanced effect. Actually, both curves exhibit a definite tendency to rise at the most forward angles. Plotting the data in the manner shown

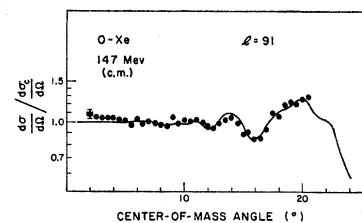


FIG. 2. Differential elastic scattering cross section relative to Coulomb vs center-of-mass angle for oxygen on xenon at 147 Mev. Error bars designate probable relative errors among experimental points. Solid curve is sharp-cutoff-model prediction for the parameters shown.

¹³ C. L. Critchfield and D. C. Dodder, *Phys. Rev.* **75**, 419 (1949).

TABLE II. Elastic scattering parameters.

Reaction	Energy (Mev)	η	l	Δl	R (10^{-13} cm)	r_0 (10^{-13} cm)
O-Xe	147	22.3	91		10.63	1.47
O-Ar	109	7.28	60	3.5	8.48	1.43
O-Ne	85	3.99	41	3	7.36	1.41

is obviously desirable for the purposes of comparison, since it is invariably relative differences from Coulomb which are of interest. However, it also has the severe disadvantage of exaggerating any errors due to angle and energy uncertainty. A further error not listed would be contributions from unresolved excited states. If important, these would cause anomalously high cross sections at the larger angles where such contributions would be largest, by percentage.

Superposed upon the datum points of Figs. 1 and 2 are the best fits obtained in terms of a sharp-cutoff calculation. A rounded-edge modification^{1,2,14} was used in the case of the argon. The parameter Δl served to damp out the oscillations normally observed in a simple Blair-type⁵ computation. Since loss of sufficient counting rate prevented carrying the xenon run into the falloff region, it was not necessary to invoke such refinements in this case. In both curves the primary feature matched in obtaining a value of l was location of the last maximum in the Coulomb plateau. Subject to this criterion, the optimum l is sensitive to within 2%. The error bars shown reflect the relative error and angle uncertainty only. The total displacement error (relative to Coulomb) should be about twice this. The parameters selected are summarized in Table II. The interaction radii R are defined by

$$E = \frac{Z_1 Z_2 e^2}{R} + \frac{\hbar^2 l(l+1)}{2\mu R^2},$$

where E is the center-of-mass energy, μ is the reduced mass of the system, and the remaining symbols have

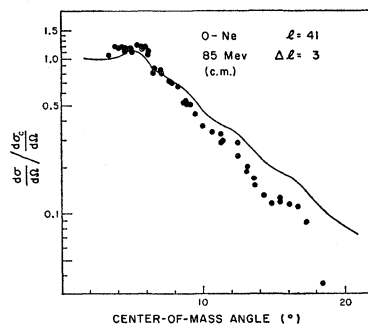


FIG. 3. Differential elastic scattering cross section relative to Coulomb vs center-of-mass angle for oxygen on neon at 85 Mev. Solid curve is diffused sharp-cutoff-model prediction for the parameters shown.

¹⁴ J. A. McIntyre, K. H. Wang, and L. C. Becker, Phys. Rev. **117**, 1337 (1960).

their usual connotation. The radius parameter r_0 is defined in the usual fashion

$$R = r_0(A_1^{1/3} + A_2^{1/3}),$$

where the A 's are the atomic numbers of the projectile and target, respectively. An average value of 131 was taken in the case of the polyatomic xenon target.

Encouraged by the satisfactory results of this analysis, the neon data of Newman¹ were re-analyzed in this same fashion, disregarding completely the relatively small-amplitude oscillatory structure. The results are shown in Fig. 3. The slight discrepancy in energy is primarily due to improved estimates of the energy loss relationships in neon. The difference is well within the estimated error. The fit is quite obviously better in over-all shape, and actually does not do too much violence to the oscillations in the experimental data. Of particular interest, however, is the greatly reduced radius parameter which results. This new value would appear to be more compatible with those obtained in other scattering reactions. The difference, however, should serve to emphasize the folly of attaching undue significance to such parameterization.

FRAGMENTATION RESULTS

The fragmentation study was performed in the manner described by Roll.⁹ The analyzed and collimated oxygen beam was scattered from a high-purity isotopically enriched Ar⁴⁰ gas target. The reaction particles were detected in a proportional counter—CsI crystal telescope.¹⁵ The former gives a signal proportional to the specific ionization loss, while the latter records the residual energy. The coincidence spectrum, when these two signals were fed respectively to the vertical and horizontal axes of an oscilloscope, resulted in a family of hyperbolic loci, each member corresponding to a given elemental species. The pulse-height spectrum was converted into energy using the known calibration curves for CsI and the range-energy curves for argon and nickel. Nominal laboratory angles of 9°, 13°, 17°, 22°, 26°, 31°, 36°, 41°, 51°, 60°, 70°, and 77° were used for these observations.

Sample spectra are shown in Fig. 4. Mainly forward-angle data have been displayed, since these show most of the structure mentioned below. The low-energy features disappear at backward angles simply from the

¹⁵ C. E. Anderson, W. J. Knox, A. R. Quinton, and G. R. Bach, Phys. Rev. Letters **3**, 557 (1959).

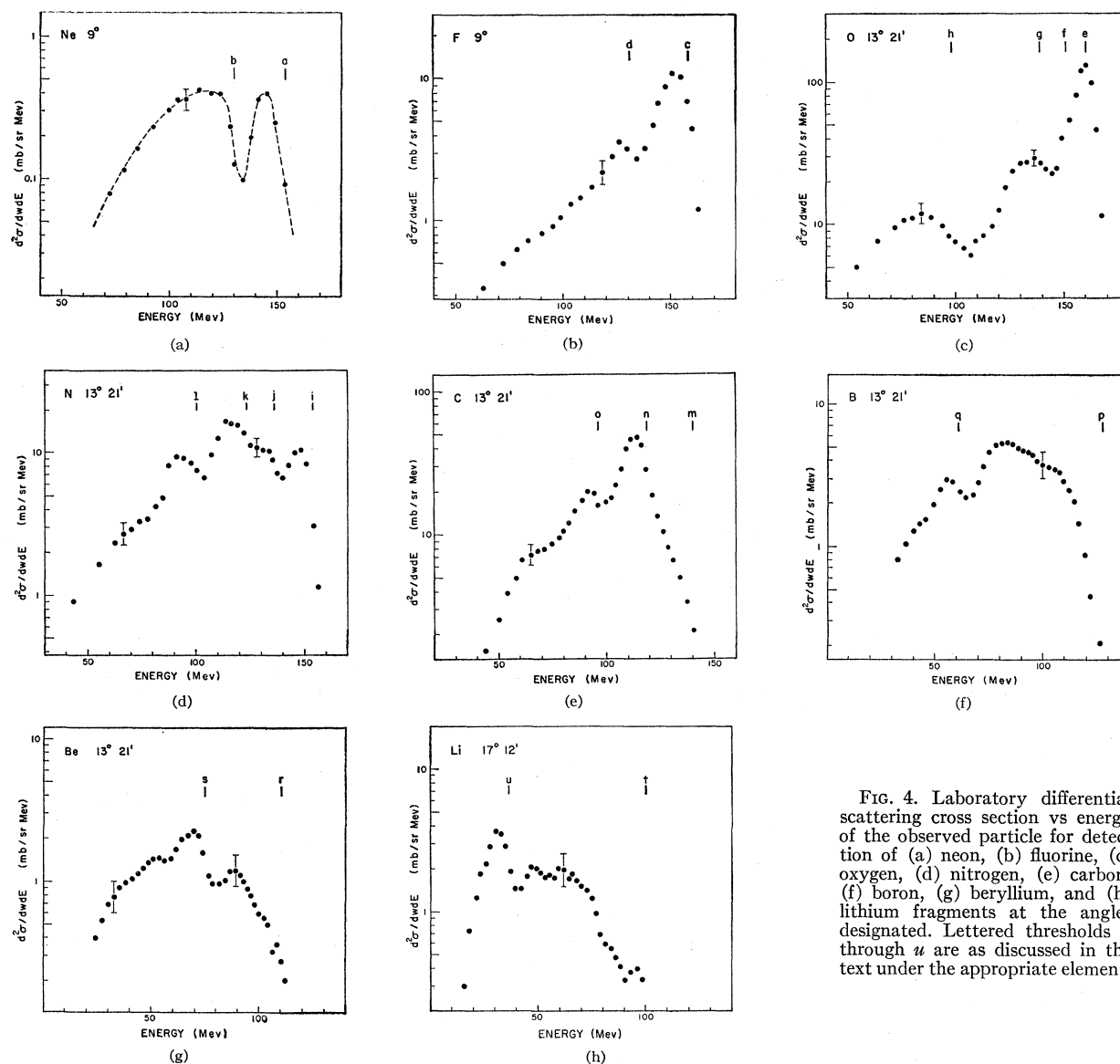


FIG. 4. Laboratory differential scattering cross section vs energy of the observed particle for detection of (a) neon, (b) fluorine, (c) oxygen, (d) nitrogen, (e) carbon, (f) boron, (g) beryllium, and (h) lithium fragments at the angles designated. Lettered thresholds *a* through *u* are as discussed in the text under the appropriate element.

center-of-mass transformations. The error bars shown are statistical. The relative smoothness of the plots is in part due to the plotting procedure used. The pulse height was analyzed in terms of 40 channels, but with each channel count considered as a Gaussian of half-width one channel. While this certainly smears out detail, it helps greatly to reduce statistical fluctuations. It is obvious that only gross features will remain. The ordinate scale is absolute in the sense that it is normalized in terms of the elastic group. However, this group is not well resolved, even at the most forward angles. The cross section should hence only be considered reliable to about a factor of 2.

In general, the spectra do not show the structure seen by Roll for the oxygen-oxygen system. However, many of the same features are repeated. In particular,

there are a number of relatively sharp thresholds which reproduce to constant *Q* value in the center-of-mass system. These are discussed below. There is also evidence of "groups" in the nitrogen and carbon spectra at velocities that would appear to correspond to formation of oxygen in the lower particle unstable states, followed respectively by proton and alpha emission in flight. The high-energy edges of the species lighter than nitrogen do not demonstrate the more precipitous thresholds observed for the heavier elements. In general they would appear to ease toward zero over a larger energy span, and even show some tendency to fall away from a constant-*Q* behavior at larger angles. Given the former, however, the latter trend is not unexpected, simply on the basis of the experimental difficulty of observing the small cross sections reliably.

Neon [Fig. 4(a)]

The sharp initial group *a* would correspond to a *Q* value of -2 Mev and is probably associated with the alpha transfer reaction $\text{Ar}^{40}(\text{O}^{16}, \text{Ne}^{20})\text{S}^{36}$, $Q = -2.004$ Mev. The relative magnitude of this structure drops rapidly with increasing angle and is only apparent as a washed-out slow rise at 26° . The secondary continuum *b* corresponds to a *Q* value of about -32 Mev for Ne^{20} observation or about -22 Mev for Ne^{24} . As the primary group weakens, this edge is not as distinct as at 9° until it takes over again at 26° and then persists out to 36° . Energetically, this edge could correspond to the binary fission of Ar^{40} into O^{16} and Ne^{24} , $Q = -24.32$ Mev.

Fluorine [Fig. 4(b)]

The sharp rise *c*, which has a *Q* value of -10 Mev for F^{18} observation and -12 Mev for F^{17} , dominates the spectrum out to 26° . At 31° and 36° it is still in evidence, but as a slow rise. It undoubtedly is comprised of the proton and deuteron transfer reactions $\text{Ar}^{40}(\text{O}^{16}, \text{F}^{17})\text{Cl}^{39}$, $Q = -11.91$ Mev and $\text{Ar}^{40}(\text{O}^{16}, \text{F}^{18})\text{Cl}^{38}$, $Q = -10.81$ Mev, respectively. The small rise apparent at *d* becomes more pronounced as the angle increases and is the primary high-energy edge from 31° out to 51° . It has a *Q* value of about -30 Mev for F^{18} observation and -34 Mev for F^{20} . Energetically it could thus correspond to the symmetric fission of Ar^{40} into two F^{20} fragments, $Q = -35.0$ Mev.

Oxygen [Fig. 4(c)]

The elastic group *e* dominates the spectrum out to 21° . The small suggestion of a shoulder at *f* with a *Q* value of about -8 Mev becomes quite pronounced at 17° and persists to 35° . It undoubtedly corresponds to the neutron transfer reactions $\text{Ar}^{40}(\text{O}^{16}, \text{O}^{15})\text{A}^{41}$, $Q = -9.55$ Mev, and $\text{Ar}^{40}(\text{O}^{16}, \text{O}^{17})\text{Ar}^{39}$, $Q = -5.698$ Mev. The broad structure at *g* with a *Q* of about -22 Mev persists out to 26° then appears to decrease slowly in energy to a *Q* of about -28 Mev at 60° . In this latter span it is the high-energy edge of the spectrum. Energetically it could be the analog group to *b* above, or also to the nitrogen group *j* following. The low-energy hump at *h*, with a *Q* value of about -60 Mev, is present out to 31° , but becomes slowly less pronounced. Energetically it could correspond to the general disintegration of the Ar^{40} target into $(2\text{O}^{16}, \alpha, 4n)$, $Q = -60.27$ Mev.

Nitrogen [Fig. 4(d)]

While much of the apparent structure shown is at the limit of the statistics, most of it is verified by its continued presence after the attenuation of its higher energy neighbors. Of particular interest is "group" *k*, which only occurs at forward angles and is strongest at 13° . Its high-energy edge would correspond in ve-

locity to an inelastic oxygen ion in the lowest proton unstable state. The edge *i*, with a *Q* value of about -8 Mev, remains relatively sharp out to 21° and is present but washed out at 26° . It undoubtedly corresponds to the proton and deuteron transfer reactions $\text{Ar}^{40}(\text{O}^{16}, \text{N}^{15})\text{K}^{41}$, $Q = -4.27$ Mev, and $\text{Ar}^{40}(\text{O}^{16}, \text{N}^{14})\text{K}^{42}$, $Q = -7.58$ Mev, respectively. The rise at *j*, with a *Q* value of -22 Mev, persists out to 41° ; it is the high-energy edge from 26° out. The rise at *l*, which has a *Q* of about -52 Mev, persists to 77° and is the high-energy cutoff from 51° back. For both latter, and most of the succeeding groups, no interpretations are presented. Plausible, but probably not unique, assignments can be constructed quite easily, but in these cases one cannot examine the spectra of the complementary fragments to check for consistency.

Carbon [Fig. 4(e)]

The relatively washed-out nature of the high-energy edge for the light elements is typified by carbon. The apparent threshold at *m* corresponds to a *Q* value of about -20 Mev. This is about what one would expect for carbon fragments from the binary fission of the argon target. It persists out to 31° and then decreases somewhat in energy (to a *Q* of -30 Mev) before it disappears after 41° . The rise at (*o*), with a *Q* of about -55 Mev, is seen at all angles and is the high-energy cutoff from 50° back to 77° . The "group" *n* is only in evidence at forward angles and is most pronounced at 13° . In velocity, its high-energy edge is consistent with the inelastic scattering of oxygen in the lower alpha unstable states with subsequent alpha emission in flight.

Boron [Fig. 4(f)]

The high-energy edge *p*, with a *Q* of about -26 Mev, persists out to 31° and then decreases in energy to about -34 Mev at 51° . The rise at *q*, with a *Q* value of about -85 Mev, appears at only the three forward angles.

Beryllium [Fig. 4(g)]

The high-energy edge *r*, with a *Q* of about -45 Mev, persists out to 50° . This much sharper rise *s* with a *Q* of about -70 Mev, is present at all angles, but moves back slightly in energy at 70° and 77° .

Lithium [Fig. 4(h)]

The rather nebulous high-energy edge (*t*), with a *Q* of about -50 Mev, remains steady out to 36° and from there gradually recedes to -80 Mev at 77° . The more precipitous rise *u*, with a *Q* of about -96 Mev, is only present out to 31° . With regard to velocity it would correspond to inelastically scattered oxygen ions excited to form an unstable cluster consisting of an alpha particle plus two Li^6 nuclei.

CONCLUSIONS

The elastic-scattering data only serve to confirm what was obviously expected. When one moves into the more classical region, as attested by the larger values of the parameter η , and restricts the discussion to sufficiently forward angles, the elastic cross section is essentially Rutherford. Further, the radius parameter, extracted from fitting mainly this forward-angle region, as opposed to the diffraction-like extrema, are reminiscent of low-energy alpha-particle-scattering results. These radii appear to be systematically, but not significantly, smaller than those obtained in the presence of diffraction-like effects. This is somewhat at odds with the tendency toward larger radii usually observed as

one goes to lower energies of the same scattering system.^{2,3}

The processes involved in the fragmentation experiment are, admittedly, rather poorly understood. The transfer reactions appear to be strong contributors at the forward angles, as is to be expected. One can only speculate on the origin of the remaining structure, however. Work is being continued on this analysis.

ACKNOWLEDGMENTS

The authors would like to acknowledge the participation of Dr. E. Newman, Dr. P. G. Roll, and Dr. A. M. Smith at various stages of the elastic-scattering work. Without their assistance it could not have been completed. Thanks are also due to Dr. P. G. Roll and Dr. C. E. Anderson for assistance in the fragmentation work.

Isotope Shift in the Spectrum of Osmium*

ARTHELLA P. HINES AND JOHN S. ROSS

Department of Physics, Rollins College, Winter Park, Florida

(Received October 27, 1961; revised manuscript received February 9, 1962)

Using enriched isotopes, the isotopic shift in five lines of the osmium spectrum, involving transitions of the type $5d^66s6p-5d^66s^2$, was measured with a Fabry-Perot interferometer. The average relative isotope shift for the even isotopic pairs, $\Delta\nu(192-190):\Delta\nu(190-188):\Delta\nu(188-186):\Delta\nu(186-184)$, was found to be 1.00:1.12:1.29:1.31, showing a leveling off in the isotope shift as the last neutron pair is subtracted. This results in a predicted intrinsic quadrupole moment for Os^{184} of $6.0 \times 10^{-24} \text{ cm}^2$. The odd-isotope shift $\Delta\nu(192-190):\Delta\nu(189-187)$ was determined to be 1.00:1.27. The average value for $\Delta\nu(190-188):\Delta\nu(190-189)$ and $\Delta\nu(188-186):\Delta\nu(188-187)$ was found to be 1.00:0.69, illustrating the usual even-odd staggering effect.

INTRODUCTION

RESULTS from experimental measurements of atomic isotope shifts provide information about the variation in the nuclear charge distribution, which results from a change in the number of neutrons in a nucleus. Osmium lies between the heavy elements lead and mercury, where the even isotopes exhibit¹ a progressively decreasing shift with decreasing mass, and hafnium and tungsten, which show^{2,3} an inversion in their even-isotope shifts. Due to its location, therefore, the isotope shift of osmium is of particular interest.

Optical examination of the osmium spectrum by several investigators,^{1,4-6} using natural samples, has shown that there is an increasing isotope shift between the even isotopes as one proceeds from atomic mass number 192 down to 186, and a pronounced even-odd

staggering effect in 189. Murakawa and his co-workers determined the nuclear spin of Os^{189} to be $\frac{3}{2}$ and found a value of the magnetic moment in agreement with the value $\mu(\text{Os}^{189}) = +0.65065 \text{ nm}$, determined⁷ by the method of nuclear induction. Murakawa⁸ assumed the nuclear spin of Os^{187} to be $\frac{1}{2}$. Steudel and his co-workers,^{9,10} using a radiogenic 100% enriched sample of Os^{187} , confirmed this value of the nuclear spin, determined $\mu(\text{Os}^{187}) = +0.0653 \text{ nm}$, and observed even-odd staggering for 187.

The availability of the enriched isotopes of osmium provides samples for better measurement of the hyperfine components due to the odd isotopes, for obtaining more accurate even isotope positions, especially 186, and for determining the location of the 184 isotope.

* Supported by a grant from the National Science Foundation.

¹ J. Blaise, theses, University of Paris, 1958.

² W. L. Barr, *J. Opt. Soc. Am.* **48**, 658 (1958).

³ J. Blaise and G. Gluck, *J. phys. radium* **20**, 466 (1959).

⁴ S. Suwa, *Phys. Rev.* **83**, 1258 (1951).

⁵ K. Murakawa and S. Suwa, *Phys. Rev.* **87**, 1048 (1952).

⁶ K. Murakawa and T. Kamei, *Phys. Rev.* **105**, 671 (1957).

⁷ H. R. Loeliger and L. R. Sarles, *Phys. Rev.* **95**, 291 (1954).

⁸ K. Murakawa, *Phys. Rev.* **98**, 1285 (1955).

⁹ G. Guthöhrlein, H. Kopfermann, G. Nöldeke, and A. Steudel, *Naturwissenschaften* **46**, 598 (1959).

¹⁰ G. Guthöhrlein, G. Nöldeke, and A. Steudel, Program of Atomic Spectroscopy Symposium, Argonne National Laboratory, June, 1961.